Int J Fract (2009) 158:81–88
DOI 10.1007/s10704-009-9367-y
© Springer Science+Business Media B.V. 2009

LETTERS IN FRACTURE AND MICROMECHANICS

MICROFIBRIL-BASED ESTIMATES OF THE BALLISTIC LIMIT OF MULTI-LAYERED FABRIC SHIELDING

T. I. Zohdi
Department of Mechanical Engineering
6195 Etcheverry Hall
University of California, Berkeley, CA, 94720-1740, USA
email: zohdi@newton.berkeley.edu

Abstract. An expression relating the dominant mechanisms for the energy loss of a projectile, as it penetrates a multilayered ballistic fabric shield, is developed. The relation is a function of the projectile mass, initial velocity and fabric microscale properties, such as microfibril stiffness and critical stretch. Using the derived expression, the number of fabric layers needed to stop a projectile is determined. The analytical result compares quite well to experiments.

Keywords: multilayered ballistic fabric, microscale properties

1 Introduction. There exist a wide range of applications for multilayered lightweight ballistic fabric, such as body armor and shielding of critical military and commercial structural components. The reader is referred to Godfrey and Rossettos (1999), Rossettos and Godfrey (2003), Roylance and Wang (1980), Taylor and Vinson (1990), Shim et al. (1995), Johnson et al. (1999), Tabiei and Jiang (1999), Kollegal and Sridharan (2000), Walker (1999), Cheeseman and Bogetti (2003), Duan et al. (2005a, 2005b, 2006), Kwong and Goldsmith (2004), Lim et al (2002, 2003), Shockey et al (2004), Tan et al (2005), Verzemnieks (2005), Zohdi (2002), Zohdi and Powell (2006) and Powell and Zohdi (2009) for a cross-sectional view of the field. For an exhaustive and comprehensive overview of all aspects of ballistic fabric, see Tabiei and Nilakantan (2008). The objective of this work is to develop a simple analytical expression which accounts for the dominant mechanisms that strip energy away from a projectile as it penetrates a multilayered ballistic fabric shield. With this expression, one can estimate the number of fabric layers needed to stop the projectile, based upon the projectile mass, initial velocity and fabric properties.

2 Stretching and rupture. We initially consider the rupture of a single "yarn" in the fabric (Figure 1). We denote ρ_o as the initial (undeformed) density of the yarn and A_o is the initial cross-sectional area. During the stretching to final rupture, the yarn is assumed to attain a linear (symmetric) velocity profile given by $(0 \leq x \leq \frac{L_o}{2})$

$$v(x) = v_p \frac{x}{\frac{L_o}{2}}, \tag{1}$$

where v_p is the velocity of the projectile (Figure 1). We assume the that contact area of the projectile/fabric is sufficiently small with respect to the target size so that it can be considered as a point-load during this stage of the analysis. Later, the dimensions of the projectile will be taken into account. By integrating the differential kinetic energy, we obtain

$$2\int_0^{\frac{L_o}{2}} \frac{1}{2}\rho_o A_o (v(x))^2\, dx = \frac{\rho_o A_o L_o}{6}(v_p)^2. \tag{2}$$

An energy balance yields

$$\underbrace{\frac{1}{2}m_p(v_p^{(i)})^2}_{\text{kinetic energy after the ith sheet}} - \underbrace{w(U^*)}_{\text{stored elastic energy}} = \underbrace{\frac{1}{2}m_p(v_p^{(i+1)})^2}_{\text{kinetic energy after the i+1 th sheet}} + \underbrace{\frac{\rho_o A_o L_o}{6}(v_p^{i+1})^2}_{\text{fabric kinetic energy}}, \tag{3}$$

where the stretch throughout the yarn (on either side of the projectile) has been approximated as being uniform, due to the assumed mode of deformation (Figure 1). The stored energy at failure is denoted $w(U^*)$, where U^* is the critical stretch ratio at failure. The stretch ratio is defined as $U \stackrel{\text{def}}{=} \frac{L}{L_o}$, where L is the stretched length and L_o is the original unstretched length. Equation 4 may be written in the form of a recursion (i=sheet number)

$$v_p^{(i+1)} = \sqrt{\alpha (v_p^{(i)})^2 - \beta}, \tag{4}$$

where

$$\alpha = \frac{m_p}{m_p + \frac{\rho_o A_o L_o}{3}} \qquad \text{and} \qquad \beta = \frac{2w(U^*)}{m_p + \frac{\rho_o A_o L_o}{3}}. \tag{5}$$

For moderate finite strains (the case here), the response of the thin one-dimensional yarn can be accurately described by a constitutive law of the form $S = \mathbb{E}E$, where S is the second Piola-Kirchhoff stress, $\mathbb{E}$ is Young's modulus and $E \stackrel{\text{def}}{=} \frac{1}{2}(U^2 - 1)$ is the Green-Lagrange strain. The quantity of interest here is the stored energy $w(U^*) = \frac{L_o A_o}{2}\mathbb{E}(\frac{(U^*)^2-1}{2})^2$ at final rupture, where $W(U^*) \stackrel{\text{def}}{=} \frac{1}{2}\mathbb{E}\left(\frac{(U^*)^2-1}{2}\right)^2$ is the stored energy per unit volume. We shall use this simple stored energy function in the analysis that follows. However, we note that other material models could easily be employed without any complication.

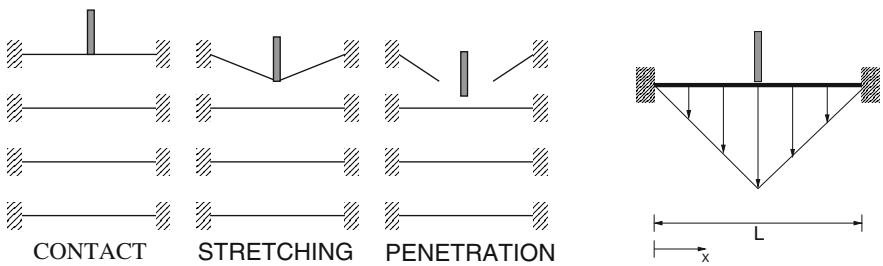

Figure 1: LEFT: Sequence of events. RIGHT: The velocity profile.

Remark 1: The axial strains, for structural fabric such as Kevlar, Spectra or Zylon, are expected to be in the range of 2 %-10 % before rupturing.[1] Therefore, a relatively simple Kirchhoff-St. Venant material model is reasonable. Although it is not explicitly needed in this analysis, the Cauchy stress (σ) is related to the second Piola-Kirchhoff stress in the following manner for this simple one-dimensional case, $\sigma = US = \sigma = \mathbb{E}\frac{U^3-U}{2}$.

Remark 2: The use of a linear velocity profile was motivated by observations in laboratory experiments and large-scale numerical studies for sheets of fabric that are clamped to a target holder (Kwong and Goldsmith (2004), Zohdi (2002), Powell et al (2008), Zohdi and Powell (2006) and Powell and Zohdi (2009)). Experimental data has been posted at http: // www.me.berkeley.edu / compmat and will be discussed later in the work.

3 Estimation of the number of sheets. By squaring both sides of Equation 4 we obtain

$$(v_p^{(i+1)})^2 = \alpha (v_p^{(i)})^2 - \beta, \tag{6}$$

and subtracting this result from the relation evaluated at the previous sheet

$$(v_p^{(i)})^2 = \alpha (v_p^{(i-1)})^2 - \beta, \tag{7}$$

yields

$$\frac{(v_p^{(i+1)})^2 - (v_p^{(i)})^2}{(v_p^{(i)})^2 - (v_p^{(i-1)})^2} = \alpha. \tag{8}$$

Therefore, the ratio of the loss of kinetic energy, $\frac{1}{2} m_p v_p^2$, from sheet to sheet, is constant and, thus,

$$(v_p^{(i+1)})^2 - (v_p^{(i)})^2 = \alpha^i \left((v_p^{(1)})^2 - (v_p^{(0)})^2 \right), \tag{9}$$

where the notation α^i denotes α to the ith power. As a result, we obtain an expression relating the sheets penetrated (i) to the velocities between layers

$$i = \frac{1}{ln\alpha} ln \left(\frac{(v_p^{(i+1)})^2 - (v_p^{(i)})^2}{(v_p^{(1)})^2 - (v_p^{(0)})^2} \right). \tag{10}$$

Setting the velocity at sheet $i+1$ to zero yields an expression for the velocity after i sheets have been penetrated,

[1] For example, Zylon ruptures at approximately a 3 % axial strain (Toyobo, 2001).

$$(v_p^{(i+1)})^2 = \alpha (v_p^{(i)})^2 - \beta = 0 \Rightarrow v_p^{(i)} = \sqrt{\frac{\beta}{\alpha}}. \tag{11}$$

Combining the two previous relations, we obtain the number of sheets (i^*) that a projectile will penetrate before stopping

$$\frac{(0)^2 - \frac{\beta}{\alpha}}{(v_p^{(1)})^2 - (v_p^{(0)})^2} = (\alpha)^i \Rightarrow i^* = \frac{1}{ln\alpha} ln \left(\frac{-\frac{\beta}{\alpha}}{(v_p^{(1)})^2 - (v_p^{(0)})^2} \right). \tag{12}$$

By applying the recursion relation to the first sheet

$$(v_p^{(1)})^2 = \alpha (v_p^{(0)})^2 - \beta \Rightarrow (v_p^{(1)})^2 - (v_p^{(0)})^2 = \alpha (v_p^{(0)})^2 - \beta - (v_p^{(0)})^2, \tag{13}$$

we obtain an expression for the number of sheets penetrated solely in terms of the system parameters and the initial velocity

$$i^* = \frac{1}{ln\alpha} ln \left(\frac{\frac{-\beta}{\alpha}}{(\alpha - 1)(v_p^{(0)})^2 - \beta} \right). \tag{14}$$

Since i^* represents the number of sheets penetrated, it should be rounded up to an integer value. Furthermore, since $i^* + 1$ represents the number of sheets needed to stop the projectile, it should also be rounded up to an integer value. Rounding the values up will provide conservative estimate in each case.

4 Experimental observations and introduction of microscale properties. The previous expressions are not specific to any particular fabric. However, for the sake of comparison to experiments, we now focus the discussion on Zylon, which is a synthetic polymer produced by the Toyobo Corporation (Toyobo, 2001) constructed from woven PBO yarn. Over the last decade, experiments conducted at UC Berkeley, initiated by the late Werner Goldsmith, have attempted to ascertain the number of sheets of Zylon needed to stop incoming projectiles. [2] The typical amount of time taken for a single (labor-intensive) ballistic test is on the order of 90 minutes, and is described in detail in Kwong and Goldsmith (2004), Zohdi (2002), Zohdi and Powell (2006), Powell et al (2008) and Powell and Zohdi (2009). In order to perform the experiments, ballistic sheets of Zylon must be cut with a pair of special scissors from a fabric roll, clamped around a circular bar and placed into a square holder. The

[2] The author gratefully acknowledges Sean Kelley, David Powell, Tim Kostka and George Mseis for providing the data at http: // www.me.berkeley.edu / compmat. Further reports, accessible to the public, can be obtained by making a request to the United States Federal Aviation Administration (FAA) indicating project 01-C-AW-WISU. For further experiments on individual yarn, see Verzemnieks (2005).

two parts of this square frame, whose outside dimensions are 356 mm with a 254 mm square window, were secured by 9.5 mm diameter hard-steel bolts via an aluminum strip, which acts as a continuous washer. After these components were assembled, this device was clamped vertically to a heavy triangular support, which was mounted onto a 700 kg steel table so that impact would be produced at a preselected location on the target, as specified by a laser beam mounted on the gun centerline. The tests were conducted using a custom-built gas gun (12.9 mm inside diameter) with a 20 mm thick high-strength steel barrel of 1.6 m length. This apparatus was mounted by means of a rail frame onto the same table as the target. The projectile consisted of a 12.7 mm diameter steel cylinder with a mass of 36 g, with an aspect ratio of 3:1 which was heat treated to a Rockwell hardness of $R_c = 60$. Also, it was copper-coated to a thickness of 0.5 mils to reduce barrel wear. A blast shield was placed in front of the muzzle to prevent interaction of ejected debri with the target. A projectile and fragment catcher, consisting of a large cloth-filled container, was positioned beyond all final velocity measuring units. The tests were conducted inside an enclosed room which was evacuated during firing. The initial velocity of the projectile was determined from the time required to successively break two parallel laser beams, 156 mm apart, which were focused on two photodiodes, located 1.5 m in front of the target. The signals from the diodes initiated the start and stop modes of a Hewlett-Packard 5316 time interval meter. Final velocities were determined in three ways: (1) by the use of a digital video recording camera, operating at 10,000 frames/s, that captured the projectile position at a number of instances after the perforation using the dimensions of the projectile, (2) by means of two silver-coated paper make-circuit grids spaced 50.4 mm apart, whose voltage pulses were directed to a time-interval meter and (3) from two sets of 432×254 mm foils, with each pair separated by 12 mm and each set a distance of 12.7 mm apart, with the projectile contact providing an "on" circuit for each set, allowing the respective signals to start and stop a time interval meter. The number of desired sheets were cut and inserted in the target holder and the bolts were tightened with a 306 N-m torque wrench. These laboratory experiments indicated that, for a projectile initially traveling at approximately 350 feet/sec (106.68 meters/sec) penetrated six (boundary) clamped sheets. Therefore, seven sheets were needed to stop the projectile. The analytical expression (Equation 14) derived earlier will now be compared to the experiments just described.

Typically, for structural fabric, the microstructure of the yarn is composed of groups of microscale fibrils. Zylon possesses such a multiscale structure, constructed from PBO (Polybenzoxale) microscale fibrils, which are bundled to form yarn, which are then tightly woven into sheets (Figure 2, Zohdi and Powell (2006)). Each yarn contains approximately 350 microfibrils. The following system parameters (from the described experiments) and standard properties of Zylon fabric (Toyobo, 2001) were used:

- mass of the projectile: $m_p \approx 0.036\, kg$,
- length of the target: $L_o \approx 0.254\, m$,
- critical stretch to failure of a Zylon micro-fibril: $U^* \approx 1.0344$ (3 % strain),
- stiffness of a Zylon microfibril: $E_f \approx 180\, GPa$,

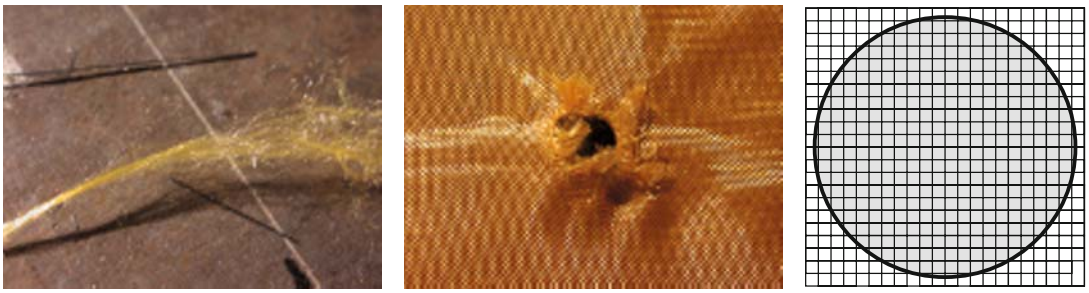

Figure 2: LEFT: The microstructure of a Zylon yarn. MIDDLE: Punctured Zylon target (Zohdi and Powell, 2006). RIGHT: Approximate determination of the total number of load-sharing yarn is determined by computing the number of yarn in the horizontal direction in contact region and the number of yarn in the vertical direction.

- radius of a Zylon microfibril: $r_f \approx 5 \times 10^{-6}\, m\, (A_f = \pi r_f^2)$,
- density of a Zylon microfibril: $\rho_o \approx 1540\, kgm^{-3}$.

The effective yarn cross-sectional area in the previous expressions is $A_o = 350 \times A_f$. Since a single yarn does not take the entire load, the stored energy and the mass of the yarn are multiplied by the number of yarn, S ("load-sharers") to compute the effective inertia and effective stored energy, yielding

$$i^* = \frac{1}{ln\alpha} ln \left(\frac{\frac{-\beta_e}{\alpha}}{(\alpha_e - 1)(v_p^{(0)})^2 - \beta_e} \right), \tag{15}$$

where $\alpha_e = \frac{m_p}{m_p + \frac{S\rho_o A_o L_o}{3}}$ and $\beta_e = \frac{2Sw(U^*)}{m_p + \frac{S\rho_o A_o L_o}{3}}$. The typical denier (yarn weave density) of a Zylon weave is 35 yarn/inch (=$35 \times (100/2.54)$ yarn/meter). In order to estimate the number yarn that share the load, for a cylindrical penetrator, such as the one used in the experiments, we take twice the diameter (yarn in the vertical and horizontal directions) of the projectile (0.0127 meters) and multiply this by the yarn per unit length (Figure 2). Thus, the number of yarn that share the load is approximately $2 \times \times 0.127 \times 35 \times (100/2.54) = 35$ and the number of fibrils is approximately $350 \times 35 = 12250$. *Inserting this data into Equation 15 yields* $i^* = 6.52$*, which asserts that approximately seven sheets (conservatively rounding up to an integer value) will be penetrated by the projectile and that eight* $(i^* + 1)$ *sheets are needed to stop the projectile. This is nearly the exact number indicated by the experiments (six sheets penetrated and seven to stop the projectile).* A primary reason for the close agreement between the analytical and experiment results is the choice of the linear velocity profile in the fully deformed configuration, which essentially matches the observed state of the fabric for clamped boundary conditions. Figure 3 illustrates the typical velocity/sheet-penetration square-root (sub-linear) behavior widely observed in ballistics studies.

5 Summary. A relation was derived to determine the number of ballistic fabric sheets needed to stop an incoming projectile. The relation is a function of projectile mass,

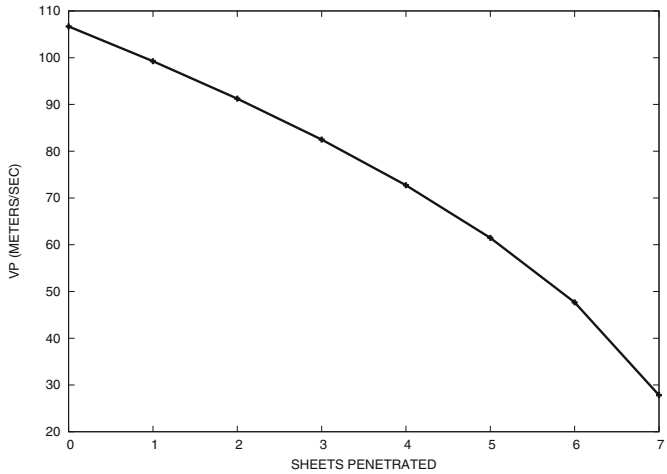

Figure 3: The velocity as a function of penetrated shields. Approximately $i^* = 6.52$ (rounded up to seven) were predicted penetrated by the theory, and $i^* + 1 = 7.52$ (rounded up to eight) were predicted to stop the projectile. This is nearly the exact number indicated by the experiments (six sheets penetrated and seven to stop the projectile).

initial velocity and microscale properties, such as microfibril stiffness and stretch to failure. The relation was compared against experiments and is in extremely close agreement. We remark that sharper estimates could be obtained by including other dissipative effects, such as friction. If we denote dissipative energy losses by $w_d \geq 0$, we can modify the recursion relation to read

$$\frac{1}{2}m_p(v_p^{(i)})^2 - w(U^*) - w_d = \frac{1}{2}m_p(v_p^{(i+1)})^2 + \frac{\rho_o A_o L_o}{6}(v_p^{i+1})^2, \tag{16}$$

leading to $v_p^{(i+1)} = \sqrt{\alpha(v_p^{(i)})^2 - \hat{\beta}}$, where $\alpha = \frac{m_p}{m_p + \frac{\rho_o A_o L_o}{3}}$ and $\hat{\beta} = \frac{2(w(U^*)+w_d)}{m_p + \frac{\rho_o A_o L_o}{3}}$ and

$$\hat{i}^* = \frac{1}{ln\alpha} ln\left(\frac{\frac{-\hat{\beta}}{\alpha}}{(\alpha-1)(v_p^{(0)})^2 - \hat{\beta}}\right). \tag{17}$$

Clearly, $i^* \geq \hat{i}^*$. The determination of w_d is non-trivial and would require estimates for the energy losses due to sliding of fabric along the projectile face, as well as intersheet contact and sliding. However, these effects appear to be somewhat small for the application under current consideration, since the Zylon and the smooth projectile surface combine to produce a low coefficient of friction.

Acknowledgements: This work was funded in part by the Federal Aviation Administration through the Aircraft Catastrophic Failure Prevention Program (cooperative agreement 01-C-AW-UCB and FAA Grant 2007-G-005), the Army Research Laboratory through the Army High Performance Computing Research Center (cooperative agreement W911NF-07-2-0027) and the Powley foundation.

References

1. Cheeseman, B. A. & Bogetti, T. A. 2003. Ballistic impact into fabric and compliant composite laminates. *Composite Structures.* **61**, 161-173.
2. Duan, Y. Keefe, M. Bogetti, T. A. Cheeseman, B. A. 2005a. Modeling the role of friction during ballistic impact of a high-strength plain-weave fabric. *Composite Structures.* **68**, 331-337.
3. Duan, Y. Keefe, M. Bogetti, T. A. Cheeseman, B. A. 2005b. Modeling friction effects on the ballistic impact behavior of a single-ply high strength fabric. *Int J of Impact Eng.* **31**, 996-1012.
4. Duan, Y. Keefe, M. Bogetti, T. A. Powers, B. 2006. Finite element modeling of transverse impact on a ballistic fabric. *Int J of Mech Sci.* **48**, 33-43.
5. Godfrey, T. A. & Rossettos, J. N. 1999. The onset of tear propagation at slits in stressed uncoated plain weave fabrics. *Journal of Applied Mechanics.* **66**, 926-933.
6. Johnson, G. R., Beissel, S. R. & Cunniff, P. M. 1999. A computational model for fabrics subjected to ballistic impact. In *Proceedings of the 18th international symposium on ballistics*, San Antonio, TX, 962-969.
7. Kollegal, M. G. & Sridharan, S. 2000. Strength prediction of plain woven fabrics. *Journal of Composite Materials.* **34**, 240-257.
8. Kwong, K. & Goldsmith, W. 2004. Lightweight Ballistic Protection of Flight-Critical Components on Commercial Aircraft - Ballistic Characterization of Zylon. FAA report DOT/FAA/AR-04/45, P1.
9. Lim, C. T. Tan, V. B. C. Cheong, C. H. 2002. Perforation of high-strength double-ply fabric system by varying shaped projectiles. *Int J of Impact Eng.* **27**, 577-591.
10. Lim, C. T. Shim, V. P. W. Ng, Y. H. 2003. Finite-element modeling of the ballistic impact of fabric armor. *Int J of Impact Eng.* **28**, 13-31.
11. Powell, D. Zohdi, T. I. & Johnson, G. 2008. Multiscale Modeling of Structural Fabric Undergoing Impact. FAA report DOT/FAA/AR-08/38.
12. Powell, D. & Zohdi, T. 2009. Attachment mode performance of network-modeled ballistic fabric shielding. Accepted into Composites Part B.
13. Rossettos, J. N. & Godfrey, T. A. 2003. Effect of slipping yarn friction on stress concentration near yarn breaks in woven fabrics. *Textile Res J.* **73**, 292-304.
14. Roylance, D. & Wang, S. S. 1980. *Penetration mechanics of textile structures, ballistic materials and penetration mechanics,* 273-293, Elsevier.
15. Shim, V. P., Tan, V. B. C. & Tay, T. E. 1995. Modelling deformation and damage characteristics of woven fabric under small projectile impact. *Int. J. Impact Engng.* **16**, 585-605.
16. Shockey, D. A. Erlich, D. C Simons, J. W. 2004. Lightweight Ballistic Protection of Flight-Critical Components on Commercial Aircraft - Large-Scale Ballistic Impact Tests and Computational Simulations. FAA report DOT/FAA/AR-04/45, P2.
17. Tabiei, A. & Jiang, Y. 1999. Woven fabric composite material model with material nonlinearity for finite element simulation. *Int. J. of Solids and Structures.* **36**, 2757-2771.
18. Tabiei, A. & Nilakantan, G. 2008. Ballistic impact of dry woven fabric composites: a review. *Applied Mechanics Reviews.* **61**, 1-13.
19. Tan, V. B. C. Shim, V. P. W. Zeng, X. 2005. Modelling crimp in woven fabrics subjected to ballistic impact. *Int J of Impact Eng.* **32**, 561-574.
20. Taylor, W. J. & Vinson J. R. 1990. Modelling ballistic impact into flexible materials. *AIAA Journal*, **28**, 2098-2103.
21. Toyobo. 2001. PBO fiber ZYLON. Report of the Toyobo Corporation, LTD, www.toyobo.co.jp.
22. Walker, J. D. 1999. Constitutive model for fabrics with explicit static solution and ballistic limit. In *Proceedings of the 18th international symposium on ballistics*, San Antonio, TX, 1231-1238.
23. Verzemnieks, J. 2005. Lightweight Ballistic Protection of Flight-Critical Components on Commercial Aircraft - Zylon Yarn Tests. FAA report DOT/FAA/AR-05/45, P3.
24. Zohdi, T. I. 2002. Modeling and simulation of progressive penetration of multilayered ballistic fabric shielding. *Computational Mechanics.* **29**, 61-67.
25. Zohdi, T. I. & Powell, D. 2006. Multiscale construction and large-scale simulation of structural fabric undergoing ballistic impact. *Computer Methods in Applied Mechanics and Engineering.* Volume 195, Issues 1-3, Pages 94-109.